DOI: 10.3901/CJME.2014.0721.121, available online at www.springerlink.com; www.cjmenet.com; www.cjmenet.com.cn

Nonlinear Dynamic Modeling for a Diesel Engine Propeller Shafting Used in Large Marines

ZHANG Qinglei[1, 2], DUAN Jianguo[2, *], ZHANG Suohuai[3], and FU Yumin[2]

1 *School of Mechanical Engineering, University of Shanghai for Science and Technology, Shanghai 200093, China*
2 *Central Academe, Shanghai Electric Group Co., Ltd, Shanghai 200070, China*
3 *School of Mechanical and Automation Engineering, Shanghai Institute of Technology, Shanghai 201418, China*

Received November 21, 2013; revised July 16, 2014; accepted July 21, 2014

Abstract: Longitudinal vibration, torsional vibration and their coupled vibration are the main vibration modes of the crankshaft-sliding bearing system. However, these vibrations of the propeller-crankshaft-sliding bearing system generated by the fluid exciting force on the propeller are much more complex. Currently, the torsional and longitudinal vibrations have been studied separately while the research on their coupled vibration is few, and the influence of the propeller structure to dynamic characteristics of a crankshaft has not been studied yet. In order to describe the dynamic properties of a crankshaft accurately, a nonlinear dynamic model is proposed taking the effect of torsional-longitudinal coupling and the variable inertia of propeller, connecting rod and piston into account. Numerical simulation cases are carried out to calculate the response data of the system in time and frequency domains under the working speed and over-speed, respectively. Results of vibration analysis of the propeller and crankshaft system coupled in torsional and longitudinal direction indicate that the system dynamic behaviors are relatively complicated especially in the components of the frequency response. For example, the 4 times of an exciting frequency acting on the propeller by fluid appears at 130 r/min, while not yield at 105 r/min. While the possible abnormal vibration at over-speed just needs to be vigilant. So when designing the propeller shafting used in marine diesel engines, strength calculation and vibration analysis based only on linear model may cause great errors and the proposed research provides some references to design diesel engine propeller shafting used in large marines.

Keywords: nonlinear dynamics, propeller shafting, marine engine, numerical simulation

1 Introduction

A propeller shafting consisting of a crankshaft, sliding bearings, a propeller, connecting rods and pistons etc. is the core component of a large-scale marine diesel engine. In the working status, the force generating from burning diesel fuel and passing through pistons, connecting rods and crankshaft drives the propeller rotation and overcomes the resistance to push a ship forward. Because of the asymmetric structure of the crankshaft, the nonlinearity reacting force of piston-rod system and the fluid-structure interaction between the propeller and fluid and so on, the propeller shafting could generate a greater nonlinear vibration which will have a strong impact on working performance of the diesel engine. At the same time, the crankshaft of the large-scale and low-speed marine diesel engine is supported by multiple bearings and connected with a propeller. Its bending stiffness is relatively high, while the longitudinal and torsional stiffness are just the opposite. Thus the lateral vibration is small, and the longitudinal vibration, torsional vibration and their coupled vibration become the major shapes. Hence it is of great significance to improve the design level of crankshaft of a large-scale marine diesel engine that building torsional-longitudinal coupled nonlinear model of a propeller shafting to study its torsional-longitudinal coupled dynamic behaviors and vibration characteristics.

A series of researches about crankshaft system and its dynamic characteristics have been done by scholars at home and abroad. DOREY[1] and POOLE[2], pointed out that the longitudinal vibration induced by torsion is multi-frequency vibration. Some early works on torsional vibrations and crankshaft models were developed in an isolated manner[3–5]. The engine was treated as a rigid block, and the gas torque and loads were considered as the prescribed functions of time.

Recently, sophisticated nonlinear models involving the coupling of the crankshaft motion on the engine block have been developed. Taking account of the variation of the system geometry with the crank angle, BRUSA, et al[6], studied the torsional vibration of crankshafts and dealt with both free behavior and response to external excitation. ASHRAFIUON, et al[7], made design optimization of

* Corresponding author. E-mail: caleb_duan@aliyun.com
Supported by Shanghai Municipal Commission of Economy and Informatization of China(Grant Nos. 201001007, 2013000016)

variable stroke compressors come true by using asymptotic analysis. MURAWSKI[8] researched longitudinal vibration characteristics of a propulsion plant of a marine power transmission system under considering torsional-longitudinal-bending coupled behaviors and boundary conditions. The results show that the foundation stiffness has a great influence on stiffness and coupling coefficient of a crankshaft. SUN, et al[9], studied the effect of lubrication status of bearing caused by crankshaft deformation on crankshaft strength for crankshaft-bearing system of internal combustion engine. Furthermore, he studied elastohydrodynamic lubrication properties of crankshaft bearings considering the whole crankshaft deformation under load and surface roughness[10–11]. ZHANG, et al[12], carried on theoretical and experimental studies on torsional vibration of an aircraft engine-propeller system and developed two system models-a rigid body model and a flexible body model for predicting torsional vibrations of the crankshaft under different engine powers and propeller pitch settings. CHARLES, et al[13], detected the crankshaft torsional vibration of diesel engines for combustion related diagnosis. KHALED, et al[14], proposed a six degree-of-freedom nonlinear dynamic model of a marine surface vessel considering the effects of inertial forces, wave excitations, retardation forces, nonlinear restoring forces, wind and current loads along with linear viscous damping terms. LIANG, et al[15], presented a method to identify the axial vibration excitation source of crankshafts for high speed diesel engines based on an auto-regressive and moving average(ARMA) model to improve the calculation reliability and identify the excitation source of axial vibration of vehicle engine crankshafts. LIANG, et al[16], presented a method to identify the root cause of the longitudinal vibration of crankshafts for high speed diesel engines based on an auto-regressive and moving average model and the analytic hierarchy process. It turns out that the axial vibration of the crankshaft is mainly coupled and excited by the bending vibration at high speeds. But at low speeds, the axial vibrations in some frequencies are coupled and excited primarily by the torsional vibration. A nonlinear torsional vibration model of a multi-cylinder crankshaft assembly of an internal combustion engine was established using the Lagrange rule by HUANG, et al[17], considering nonlinear factors such as the non-constant inertia of reciprocating components and the structural damping of shaft segments. The results show that the non-constant inertia is an important factor of nonlinear vibration of a crankshaft. BELLAKHDHARA, et al[18], proposed a model based on beam theory with consideration of several considerations including bearing misalignments, crankshaft bending stiffness, clearance, hydrodynamic sustention and bearing deformation stiffness. The model substitutes efficiently engine simulation in crankshaft and bearing preliminary design. LEE, et al[19], described a theoretical analysis of a hydrostatic journal bearing for a crankshaft pin turner by considering the waviness error of the journal and bearing. The load carrying capacity varies according to the amplitude and phase angle of the waviness functions, and the influence of the waviness error is a significant factor in analyzing lubrication characteristics. LIN, et al[20], used hydrodynamic lubrication coupling multi-body dynamic system for simulation to reflect the engine's actual working conditions and found that engine crankshaft system's oil film dynamic lubricating friction has certain impact on system's dynamic characteristics, and the oil film dynamic lubricating friction behavior of the system should be considered in dynamic simulation calculations.

It can be seen from the above analysis that the torsional and longitudinal vibration has been researched separately while the research on their coupled vibration is few, and the influence of the propeller structure to dynamic characteristics of a crankshaft has not been studied yet. The torsional-longitudinal coupled nonlinear model of a crankshaft-bearing-piston-rod-propeller system is established using mass centralized method and considering the influence factors of the asymmetric structure of a crankshaft, the non-constant inertia of connecting rod and piston, the structure of a propeller and the fluid-structure interaction between a propeller and water etc. to improve the crankshaft structural design of a large-scale and low-speed marine diesel engine in this paper.

2 Variable Inertia Calculation

A crankshaft coordinate system is shown in Fig. 1.

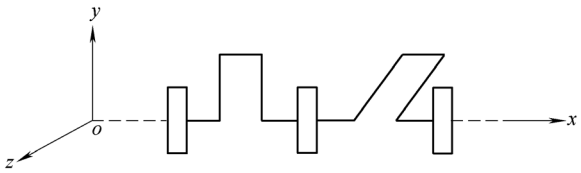

Fig. 1. Crankshaft coordinate system

As shown in Fig. 2, original angle between n cranks and xoy plane are denoted as $\varphi_1, \varphi_2, \cdots, \varphi_I, \cdots, \varphi_n$ respectively.

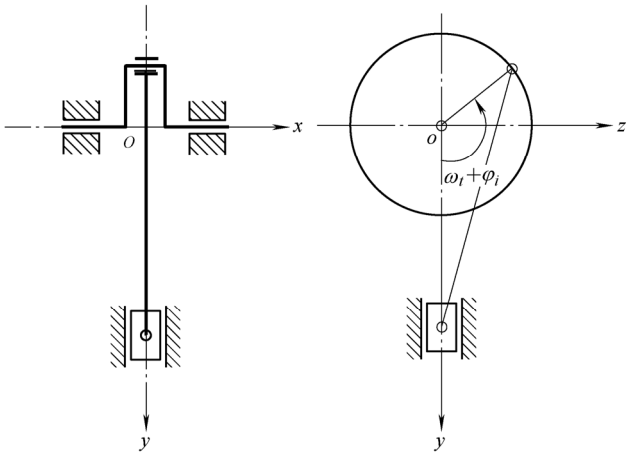

Fig. 2. Original angle between crankshaft and xoy plane

2.1 Equivalent mass and moment of inertia

Below rules are obeyed when calculating the equivalent mass and equivalent moment of inertia caused by the rotation of crankshaft.

(1) Keeping the centroid unchanged while allocating the mass of the connecting rod to both ends.

(2) Keeping the mass, centroid and moment of inertia unchanged while allocating the mass of crankshaft to the journal of the bigger end and the main journal of the crankshaft.

(3) Ignoring the friction.

(4) Assuming the crankshaft and piston as rigid bodies and ignoring their elastic deformation.

A group of crankshaft, connecting rod and piston was selected randomly as shown in Fig. 3. After allocating the connecting rod mass to both ends, M_A, M_B and the moment of inertia around A are calculated by

$$M_A = \frac{l_B}{l} m_l, \tag{1}$$

$$M_B = \frac{l_A}{l} m_l, \tag{2}$$

$$I_A = \left(\frac{r_1}{r} m_r + \frac{l_B}{l} m_l\right) r^2, \tag{3}$$

where 1, 2, 3, 4 denote frame, crankshaft, connecting rod and piston respectively and O, B and A are the center of rotation, the piston position and the center of connecting rod journal respectively. r is the crankshaft turning radius, W is the distance between crankshaft centroid and center of rotation O_{r1}, m_r is the mass of crankshaft, l is the length of connecting rod, l_A is the distance between the centroid of connecting rod G and its center of journal A, l_B is the distance between G and B, m_l is the mass of connecting rod, m_B is the mass of the piston, ω *is* the rotation speed.

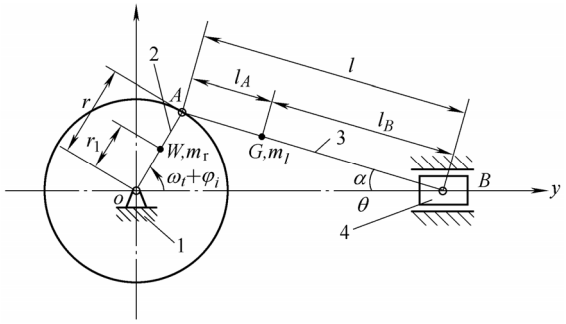

Fig. 3. Equivalent mass and moment of inertia of crankshaft

Moment of inertia of the crank-connecting rod mechanism is approximately written as[16]

$$I(\omega t+\varphi) = I_0\left[1-\frac{r}{l}\cos 2(\omega t+\varphi)\right], \tag{4}$$

where $I_0=I_A+Mr^2/2$, $M=m_B+l_A m_l/l$, r represents crankshaft radius and $\omega t+\varphi$ is the angle between the crankshaft and the moving direction of the piston, φ is the original phase and l as the length of the connecting rod.

The connecting rod unit moment of inertia I_A includes its equivalent mass allocated to the crankshaft $m_l l_B/l$ and its unit mass M includes its equivalent mass allocated to the piston $m_l l_A/l$. The variable parameter of inertia is generally written as $\beta=r/l$.

2.2 Inertia force of the slider's reciprocating movement

As shown in Fig. 3, the displacement of slider B on y direction is given by

$$y_B = r\cos(\omega t+\varphi_i)+l\cos\alpha, \tag{5}$$

considering

$$\cos\alpha = \sqrt{1-\left(\frac{r}{l}\right)^2 \sin^2(\omega t+\varphi_i)}, \tag{6}$$

replacing it in Eq. (5), yields

$$y_B = r\cos(\omega t+\varphi_i)+l\sqrt{1-\left(\frac{r}{l}\right)^2 \sin^2(\omega t+\varphi_i)}. \tag{7}$$

Taking the derivative of Eq. (7) with respect to ω, we obtain

$$\ddot{y}_B = -r\omega^2\cos(\omega t+\varphi_i) - \frac{\omega^2 r^2\cos 2(\omega t+\varphi_i)}{\sqrt{l^2-r^2\sin^2 2(\omega t+\varphi_i)}} - \frac{\omega^2 r^4\cos^2 2(\omega t+\varphi_i)}{4\sqrt{\left(l^2-r^2\sin^2 2(\omega t+\varphi_i)\right)^3}}. \tag{8}$$

The inertia force of the reciprocating object can be obtained from acceleration of slider B multiplied by its mass M.

Plenty of actual vibration phenomenon shows that the torsional vibration of the crankshaft system usually cause longitudinal vibration, the frequency of which is twice of the torsional vibration. However, according to linear dynamics, response frequency equals exciting frequency, that is, the internal or external exciting factor can only cause synchronous vibration of the crankshaft system. Thus the frequency-doubled torsional-longitudinal vibration falls in the category of nonlinear dynamics. Additionally, due to the slight deflection of the crank pin and the deviation from the main axis caused by torsion, the crankshaft system usually shortens in the longitudinal direction with torsional deformation under the impact of forward and reverse torque.

Fig. 4 shows the force analysis of the piston. F_g represents the force on the piston by the connecting rod, P_g

is the thrust force on the piston of the gas burning, F_{g14} is the force on the piston by the cylinder liner, a_B is the acceleration of the piston, thus the inertia force can be written as $m_B a_B$ where $a_B = \ddot{y}_B$.

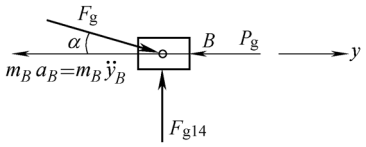

Fig. 4. Force analysis of the piston

Based on equilibrium condition of forces on the piston, we obtain

$$F_g = \frac{P_g + m_B \ddot{y}_B}{\cos\alpha}. \tag{9}$$

$\boldsymbol{R}_A$ represents the radius vector connecting an initial point A with a terminal point-the center of journal of connecting rod (as shown in Fig. 3), and $\boldsymbol{i}$, $\boldsymbol{j}$ are unit vectors in the direction of y, z coordinates, thus $\boldsymbol{R}_A$ can be written as

$$\boldsymbol{R}_A = r\cos(\omega t + \varphi_i)\boldsymbol{i} + r\sin(\omega t + \varphi_i)\boldsymbol{j}, \tag{10}$$

$$a_A = \ddot{\boldsymbol{R}}_A = -r\omega^2\cos(\omega t + \varphi_i)\boldsymbol{i} - r\omega^2\sin(\omega t + \varphi_i)\boldsymbol{j}. \tag{11}$$

The torque of the crankshaft induced by the force of the connecting rod is shown in the following equation:

$$M_t = \frac{P_g + m_B \ddot{y}_B}{\cos\alpha} r\sin(\omega t + \varphi_i + \alpha). \tag{12}$$

3 Dynamic Modeling for Crankshaft System

In convenience of research, a nonlinear model of unit crankshaft is created before the establishment of the nonlinear dynamic model of the propeller shafting system.

3.1 Equivalent longitudinal force

Fig. 5 shows a unit crankshaft system. When forced by radial force P_r, the crank pin yields bending deformation and causes the rotation of the crankshaft and the displacement of the main journal.

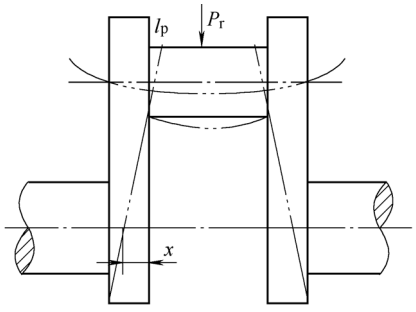

Fig. 5. Deformation of unit crankshaft

According to material mechanics, the longitudinal displacement of the 2 main journals can be expressed as

$$x = \frac{rP_r l_p^2}{16EI}, \tag{13}$$

where l_p represents the length of crank pin, r *is* the radius of crank, EI is the bending stiffness of the crank pin and P_r is the radial force.

Assuming k_l is longitudinal stiffness of the unit crank, the equivalent longitudinal force caused by P_r can be written as

$$\begin{aligned} P_l &= 2xk_l, \\ P_l &= k_l \frac{rP_r l_p^2}{8EI}. \end{aligned} \tag{14}$$

3.2 Gas load analysis

As shown in Fig. 6, the component force in the direction of the connecting rod F_g caused by the force on the piston of the cylinder can be written as

$$F_g = \frac{P_g}{\sqrt{1 - \left[\frac{r}{l}\sin(\omega t + \varphi)\right]^2}}. \tag{15}$$

And the radial force, tangential force and torque are expressed as follows:

$$P_r = P_g \frac{\cos(\omega t + \varphi + \alpha)}{\cos\alpha},$$

$$P_t = P_g \frac{\sin(\omega t + \varphi + \alpha)}{\cos\alpha},$$

$$M_t = rP_g \frac{\sin(\omega t + \varphi + \alpha)}{\cos\alpha}.$$

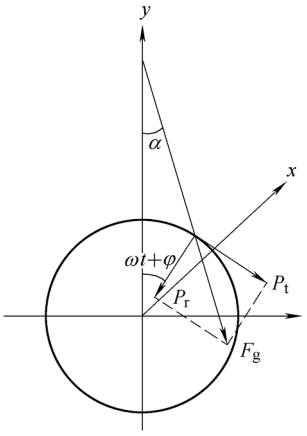

Fig. 6. Unit crank system dynamics analysis

With the assumption of $\tan\alpha = 0$, the above equations can be re-written as

$$P_r = P_g \cos(\omega t + \varphi), \tag{16}$$

$$P_t = P_g \sin(\omega t + \varphi), \tag{17}$$

$$M_t = rP_g \sin(\omega t + \varphi). \tag{18}$$

3.3 Dynamic model of unit crank system

Fig. 7 shows a unit crankshaft system consisting of a propeller, a unit crank and a mass disk. This section analyzes the torsional vibration response of the propeller and the mass disk θ_1, θ_2 or θ_1-θ_2 and longitudinal vibration response x_1, x_2 or x_1-x_2. k_l and k_t denote longitudinal stiffness and torsional stiffness respectively. Angular velocity ω and coordinate x have identical direction. Assume that the fluid resistance moment on the propeller M_m has verse direction with ω, which usually hinder the rotation of the crankshaft. Denote P_m as the fluid coupled force with damping component, M_t as the driving torque by gas explosion and P_r as the radial force. Bordered by the bearing between the propeller and crankshaft, the left segment(propeller) is simplified as m_1 and I_1, and the right segment(crankshaft and mass disk) as m_2 and I_2.

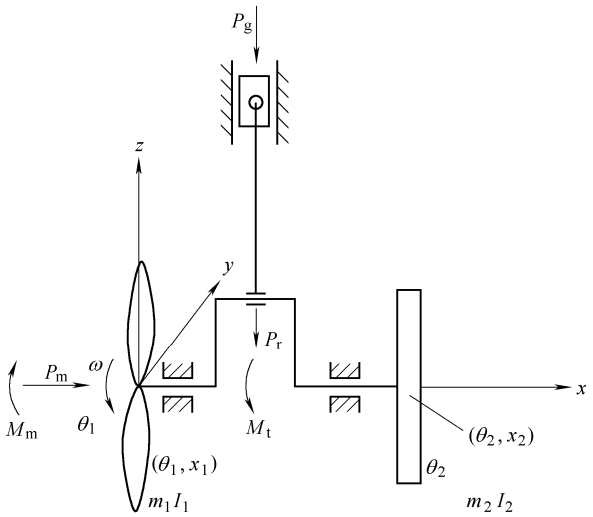

Fig. 7. Dynamic model of unit propeller-crank-shaft system

Since the variable inertia is induced by the reciprocating movement of the connect rod and the piston, only the mass of the crank is taken into consideration as constant and simplified into mass disk m_2 during the research of the longitudinal vibration. The crankshaft's longitudinal stiffness k_l and torsional stiffness k_t are calculated with its center as the border. Torsional stiffness should be taken into consideration when attached with propeller.

Assuming k_{tl} as longitudinal-torsional stiffness and k_{lt} as torsional-longitudinal stiffness, according to Fig. 7, the balance condition of the force and torque are

$$I_1\ddot{\theta}_1 + k_t(\theta_1 - \theta_2) - k_{tl}\,\mathrm{sgn}(\theta_1 - \theta_2)(x_1 - x_2) = M_m,$$

$$m_1\ddot{x}_1 + k_l(x_1 - x_2) - k_{lt}\,\mathrm{sgn}(\theta_1 - \theta_2)(\theta_1 - \theta_2) = P_m,$$

$$I_2\ddot{\theta}_2 + k_t(\theta_2 - \theta_1) + k_{tl}\,\mathrm{sgn}(\theta_2 - \theta_1)(x_2 - x_1) = M_t,$$

$$m_2\ddot{x}_2 + k_l(x_2 - x_1) + k_{lt}\,\mathrm{sgn}(\theta_2 - \theta_1)(\theta_2 - \theta_1) = P_l, \tag{19}$$

$$\mathrm{sgn}(\theta_1 - \theta_2) = \begin{cases} 1, & (\theta_1 - \theta_2) > 0, \\ 0, & (\theta_1 - \theta_2) = 0, \\ -1, & (\theta_1 - \theta_2) < 0; \end{cases}$$

$$\mathrm{sgn}(\theta_2 - \theta_1) = \begin{cases} 1, & (\theta_2 - \theta_1) > 0, \\ 0, & (\theta_2 - \theta_1) = 0, \\ -1, & (\theta_2 - \theta_1) < 0, \end{cases}$$

where P_l is the equivalent longitudinal force on the crankshaft through the piston and the connecting rod by the compressed gas in the cylinder.

After further finishing, the equations can be written as

$$\begin{cases} \ddot{\theta}_1 + \dfrac{k_t}{I_1}(\theta_1 - \theta_2) - \dfrac{k_{tl}}{I_1}\mathrm{sgn}(\theta_1 - \theta_2)(x_1 - x_2) = \dfrac{M_m}{I_1}, \\ \ddot{x}_1 + \dfrac{k_l}{m_1}(x_1 - x_2) - \dfrac{k_{lt}}{m_1}\mathrm{sgn}(\theta_1 - \theta_2)(\theta_1 - \theta_2) = \dfrac{P_m}{m_1}, \\ \ddot{\theta}_2 + \dfrac{k_t}{I_2}(\theta_2 - \theta_1) + \dfrac{k_{tl}}{I_2}\mathrm{sgn}(\theta_2 - \theta_1)(x_2 - x_1) = \dfrac{M_t}{I_2}, \\ \ddot{x}_2 + \dfrac{k_l}{m_2}(x_2 - x_1) + \dfrac{k_{lt}}{m_2}\mathrm{sgn}(\theta_2 - \theta_1)(\theta_2 - \theta_1) = \dfrac{P_l}{m_2}; \end{cases}$$

$$\begin{cases} (\ddot{\theta}_2 - \ddot{\theta}_1) + \left(\dfrac{k_t}{I_2} + \dfrac{k_t}{I_1}\right)(\theta_2 - \theta_1) + \\ \left(\dfrac{k_{tl}}{I_2} + \dfrac{k_{tl}}{I_1}\right)\mathrm{sgn}(\theta_2 - \theta_1)(x_2 - x_1) = \dfrac{M_t}{I_2} - \dfrac{M_m}{I_1}, \\ (\ddot{x}_2 - \ddot{x}_1) + \left(\dfrac{k_l}{m_2} + \dfrac{k_l}{m_1}\right)(x_2 - x_1) + \\ \left(\dfrac{k_{lt}}{m_2} + \dfrac{k_{lt}}{m_1}\right)\mathrm{sgn}(\theta_2 - \theta_1)(\theta_2 - \theta_1) = \dfrac{P_l}{m_2} - \dfrac{P_m}{m_1}. \end{cases} \tag{20}$$

Let β_1=θ_2−θ_1, y_1=x_2−x_1, Eq. (20) can be expressed as follows:

$$\begin{cases} \ddot{\beta}_1 + k_{tl}\left(\dfrac{1}{I_2} + \dfrac{1}{I_1}\right)\mathrm{sgn}(\beta_1)y_1 + k_t\left(\dfrac{1}{I_2} + \dfrac{1}{I_1}\right)\beta_1 = \\ \left(\dfrac{M_t}{I_2} - \dfrac{M_m}{I_1}\right), \\ y_1 + k_{lt}\left(\dfrac{1}{m_2} + \dfrac{1}{m_1}\right)\mathrm{sgn}(\beta_1)\beta_1 + k_l\left(\dfrac{1}{m_2} + \dfrac{1}{m_1}\right)y_1 = \\ \left(\dfrac{P_l}{m_2} - \dfrac{P_m}{m_2}\right); \end{cases} \tag{21}$$

$$\mathrm{sgn}(\beta_1) = \begin{cases} 1, & \beta_1 > 0, \\ 0, & \beta_1 = 0, \\ -1, & \beta_1 < 0. \end{cases} \tag{22}$$

P_{l} includes the inertia force induced by the reciprocating movement. Denote m_{h} as mass of the piston and the equivalent mass on it, and then the inertia force induced by the piston's reciprocating movement is

$$P_{\mathrm{h}} = m_{\mathrm{h}}\ddot{x}_B, \tag{23}$$

where x_B represents the displacement of the piston reciprocating movement.

3.4 Dynamic model of multi-crank system

Fig. 8 shows a 6-crank propeller-crankshaft system. referring to the previous nonlinear dynamic modeling method for the unit propeller-crankshaft system, the dynamic equation on point i is written as

$$\begin{cases} \ddot{\beta}_i + k_{\mathrm{t}i}\left(\dfrac{1}{I_{i+1}}+\dfrac{1}{I_i}\right)\beta_i - \dfrac{k_{\mathrm{t}(i-1)}}{I_i}\beta_{i-1} - \dfrac{k_{\mathrm{t}(i+1)}}{I_{i+1}}\beta_{i+1} + \\ k_{\mathrm{tl}i}\left(\dfrac{1}{I_{i+1}}+\dfrac{1}{I_i}\right)\mathrm{sgn}(\beta_i)y_i - \dfrac{k_{\mathrm{tl}(i+1)}}{I_{i+1}}\mathrm{sgn}(\beta_{i+1})y_{i+1} - \\ \dfrac{k_{\mathrm{tl}(i-1)}}{I_i}\mathrm{sgn}(\beta_{i-1})y_{i-1} = \dfrac{M_{t(i+1)}}{I_{i+1}} - \dfrac{M_{ti}}{I_i}, \\ \ddot{y}_i + k_{\mathrm{l}i}\left(\dfrac{1}{m_{i+1}}+\dfrac{1}{m_i}\right)y_i - \dfrac{k_{\mathrm{l}(i-1)}}{m_i}y_{i-1} - \dfrac{k_{\mathrm{l}(i+1)}}{m_{i+1}}y_{i+1} + \\ k_{\mathrm{tl}i}\left(\dfrac{1}{m_{i+1}}+\dfrac{1}{m_i}\right)\mathrm{sgn}(\beta_i)\beta_i - \dfrac{k_{\mathrm{tl}(i+1)}}{m_{i+1}}\mathrm{sgn}(\beta_{i+1})\beta_{i+1} - \\ \dfrac{k_{\mathrm{tl}i-1}}{m_i}\mathrm{sgn}(\beta_{i-1})\beta_{i-1} = \dfrac{P_{\mathrm{t}(i+1)}}{m_{i+1}} - \dfrac{P_{ti}}{m_i}, \end{cases} \tag{24}$$

where $M_{\mathrm{t1}}=M_{\mathrm{m}}$, $P_{\mathrm{l1}}=P_{\mathrm{m}}$, $\beta_i=\theta_{i+1}-\theta_i$, $y_{i+1}=x_{i+1}-x_i$, i=2–5.

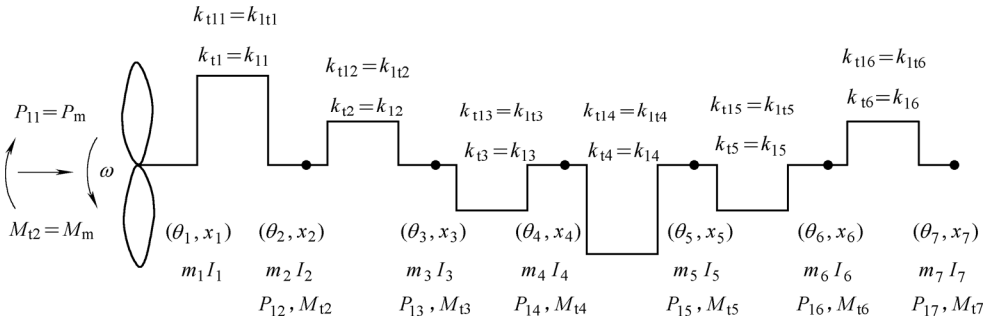

Fig. 8. Dynamic model of multi-crank system

When i=1, the dynamic equation of point 1(propeller) can be expressed as

$$\begin{cases} \ddot{\beta}_1 + k_{\mathrm{t1}}\left(\dfrac{1}{I_2}+\dfrac{1}{I_1}\right)\beta_1 - \dfrac{k_2}{I_2}\beta_2 - \dfrac{k_{\mathrm{tl2}}}{I_2}\mathrm{sgn}(\beta_2)y_2 + \\ \quad k_{\mathrm{tl2}}\left(\dfrac{1}{I_2}+\dfrac{1}{I_1}\right)\mathrm{sgn}(\beta_1)y_1 = \dfrac{M_{\mathrm{t}(i+1)}}{I_{i+1}} - \dfrac{M_{\mathrm{t}i}}{I_i}, \\ \ddot{y}_1 + k_{\mathrm{l1}}\left(\dfrac{1}{m_2}+\dfrac{1}{m_1}\right)y_1 - \dfrac{k_{12}}{m_2}y_2 - \dfrac{k_{\mathrm{tl2}}}{m_2}\mathrm{sgn}(\beta_2)\beta_2 + \\ \quad k_{\mathrm{tl2}}\left(\dfrac{1}{m_2}+\dfrac{1}{m_1}\right)\mathrm{sgn}(\beta_1)\beta_1 = \dfrac{P_{\mathrm{t2}}}{m_2} - \dfrac{P_{\mathrm{t1}}}{m_1}. \end{cases} \tag{25}$$

When i=6, the dynamic equation is transformed as follows:

$$\begin{cases} \ddot{\beta}_6 + k_{\mathrm{t6}}\left(\dfrac{1}{I_7}+\dfrac{1}{I_6}\right)\beta_6 + k_{\mathrm{tl6}}\left(\dfrac{1}{I_7}+\dfrac{1}{I_6}\right)\mathrm{sgn}(\beta_6)y_6 - \\ \quad \dfrac{k_{\mathrm{t5}}}{I_6}\beta_5 - \dfrac{k_{\mathrm{tl5}}}{I_6}\mathrm{sgn}(\beta_5)y_5 = \dfrac{M_{\mathrm{t7}}}{I_7} - \dfrac{M_{\mathrm{t6}}}{I_6}, \\ \ddot{y}_6 + k_{\mathrm{l6}}\left(\dfrac{1}{m_7}+\dfrac{1}{m_6}\right)y_6 + k_{\mathrm{tl6}}\left(\dfrac{1}{m_7}+\dfrac{1}{m_6}\right)\mathrm{sgn}(\beta_6)\beta_6 - \\ \quad \dfrac{k_{\mathrm{l5}}}{m_6}y_5 - \dfrac{k_{\mathrm{tl5}}}{m_6}\mathrm{sgn}(\beta_5)\beta_5 = \dfrac{P_{\mathrm{t7}}}{m_7} - \dfrac{P_{\mathrm{t6}}}{m_6}, \end{cases} \tag{26}$$

where

$$\mathrm{sgn}(\beta_i) = \begin{cases} 1, & \beta_i > 0, \\ 0, & \beta_i = 0, \\ -1, & \beta_i < 0. \end{cases}$$

Combining Eqs. (24), (25) and (26), the nonlinear dynamic equation of the crankshaft system with propeller can be obtained as

$$\boldsymbol{M}\ddot{\boldsymbol{X}} + \boldsymbol{C}\dot{\boldsymbol{X}} + \boldsymbol{K}\boldsymbol{X} = \boldsymbol{F}, \tag{27}$$

where the mass matrix $\boldsymbol{M}$ is a unit matrix, damping matrix $\boldsymbol{C}$ is a diagonal matrix which mainly considers the damping properties of material, stiffness matrix $\boldsymbol{K}$ is a band matrix, the elements of which are functions of time, longitudinal displacement and torsional displacement, and column vector of displacement $\boldsymbol{X}$=[$\beta_1, y_1, \beta_2, y_2, \cdots, \beta_6, y_6$].

It is a fairly complicated nonlinear dynamic system in which the mass and rotation inertia indicates periodical variation with the rotation angle of the crankshaft. Sign function sgn couples the longitudinal and torsional vibration together, hence the segment of elastic force in the dynamic equation includes a nonlinear function which makes the dynamic system a strong nonlinear and non-autonomous one. In the lack of mathematic methods, this kind of system can only be approximately solved with the help of numerical calculation method.

Eq. (27) can be transferred to state equation, where

$$\boldsymbol{A}=\begin{pmatrix}\boldsymbol{0} & \boldsymbol{M}\\ \boldsymbol{K} & \boldsymbol{0}\end{pmatrix},\quad \boldsymbol{B}=\begin{pmatrix}\boldsymbol{K} & \boldsymbol{0}\\ \boldsymbol{0} & -\boldsymbol{K}\end{pmatrix},$$
$$\boldsymbol{y}=\begin{pmatrix}x\\ \dot{x}\end{pmatrix},\quad \dot{\boldsymbol{y}}=-\frac{\boldsymbol{B}}{\boldsymbol{A}}y+\frac{1}{\boldsymbol{A}}\begin{pmatrix}\boldsymbol{F}\\ \boldsymbol{0}\end{pmatrix}. \tag{28}$$

As shown in Fig. 9, for the 6-crank propeller-crankshaft system used in marine diesel engine with high power and low speed, due to the phase difference of the force on each piston during the working process of the multi-cylinder propeller system, the exciting force on the right of Eqs. (23), (24) and (25) are expressed as

$$M_{\mathrm{t}i}=rP_{\mathrm{g}}\sin(\omega t+\varphi_i^0), \tag{29}$$

$$P_{\mathrm{r}i}=P_{\mathrm{g}}\cos(\omega t+\varphi_i^0), \tag{30}$$

$$P_{\mathrm{l}i}=k_{\mathrm{l}i}\frac{rl_{\mathrm{p}}^2P_{\mathrm{r}i}}{8(EI)_i}, \tag{31}$$

$$P_{\mathrm{h}i}=m_{\mathrm{h}i}\ddot{x}_{Bi}, \tag{32}$$

where $(EI)_i$ represents the bending stiffness of the crank pin, r is the rotation radius of the crank, l_{p} is the length of the crank pin, $P_{\mathrm{r}i}$ is the radical force on the crankshaft by the cylinder pressure, P_{g} is the pressure on the piston and φ_i is the phase difference which is 0, $2\pi/3$, $4\pi/3$, π, $-\pi/3$, $+\pi/3$ respectively, i=1–6.

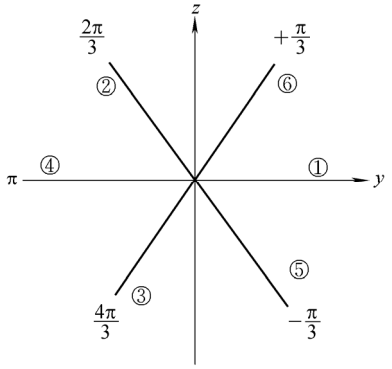

Fig. 9. Phase difference of 6-crank propeller-crankshaft system

$m_{\mathrm{h}i}$ includes the equivalent mass l_Am_l/l on the piston pin by the connecting rod. The variable inertia of all the crank-connecting rod mechanisms and the acceleration of the piston x_{Bi} are expressed as follows:

$$\ddot{x}_{Bi}=-r\omega^2\cos(\omega t+\varphi_i^0)-\frac{\omega^2r^2\cos 2(\omega t+\varphi_i^0)}{\sqrt{l^2-r^2\sin^2(\omega t+\varphi_i^0)}}-\frac{\omega^2r^4\sin^2 2(\omega t+\varphi_i^0)}{4\sqrt{\left[l^2-r^2\sin^2(\omega t+\varphi_i^0)\right]^3}}, \tag{33}$$

$$I_i=I_o\left[1-\frac{r}{l}\cos 2(\omega t+\varphi_i^0)\right]. \tag{34}$$

4 Nonlinear Vibration Analysis

4.1 Model parameters

Fig. 8 is the diagram of propeller-crankshaft system used in this section and Eq. (28) is the corresponding equation for nonlinear dynamic analysis. The system parameters are defined as below.

(1) Equivalent rotation inertia of all crankshaft units (kg • m^2): I_0=[51 116.565; 10 704.29; 10 704.29; 10 704.29; 10 704.29; 10 704.29; 7 735.595];

(2) Rotation radius of crankshaft(m): r=1.2;

(3) Length of connecting rod(m): l=2.628;

(4) Length of connecting rod's journal(m): l_{p}=0.194;

(5) Diameter of connecting rod's journal(m): d_{p}=0.720;

(6) Elastic modulus(N/m^2): E=2.06×10^{11};

(7) Torsional stiffness of crankshaft(N·m): $k_{\mathrm{t}i}$= [0.269 4; 6.45; 6.45; 6.45; 6.45; 3.951 4]×10^8;

(8) Longitudinal stiffness of crankshaft(N • m): $k_{\mathrm{l}i}$= [4.017 4; 4.55; 4.55; 4.55; 4.55; 4.54]×10^8;

(9) Coupled torsional-longitudinal stiffness of crankshaft (N): $k_{\mathrm{tl}i}$=[5.25; 5.25; 5.25; 5.25; 5.25; 5.25]×10^8;

(10) Equivalent mass of all crankshaft units(kg): m_i= [25 751; 15 077; 10 407; 10 407; 10 407; 10 407; 24 860];

(11) Equivalent moving mass of connecting rod and piston(kg): m_{hi}=1530;

(12) Material density(kg/m^3): ρ=7850.

Other parameters changing with time, the angular displacement of the crankshaft, the alternating equivalent inertia force of the piston and the connecting rod can be calculated with the formulas in section 2.

The technical parameters of a large low-speed two-stroke marine diesel engine MANB&6S60MC are as below: 6 cylinders, stroke 2.292 m, rated power 12 240 kW, rated speed 105 r/min. The curve of its gas pressure indicator diagram when fully loaded can be fitted through Fourier expansion. Contributing the most to the exciting torque, the first two of the expansion, summing together, is regarded as the approximate wave function of gas pressure (ignoring the rigid displacement of the shafting induced by the mean value of gas pressure) and the gas pressure of the cylinder can be written as

$$F_g=2\,683\,746\cos(\omega t)+1\,741\,897\cos(2\omega t)+509\,476\sin(\omega t)+631\,125\sin(2\omega t). \tag{35}$$

Working in certain non-uniform wake field, the fluid longitudinal thrust can be accurately obtained with the quasi-steady theory. In the lack of the data of the wake field, the longitudinal thrust P_m and torque M_m can be calculated by empirical formula[21]:

$$P_m=203\,800\cos(\omega t)+132\,280\cos(2\omega t)+38\,688\sin(\omega t)+47\,926\sin(2\omega t), \tag{36}$$

$$M_{\mathrm{m}} = -3\,218\,883\cos(4\omega t). \tag{37}$$

4.2 Dynamic response to the gas excitation

4.2.1 Response analysis at working speed

In order to make comparison with the fluid exciting behaviors, the force and torque on the propeller are assumed as zero and the physical and mechanical properties, such as the mass, rotation inertia and torsional stiffness of the propeller assumed unchanged when researching the exciting behaviors from cylinder pressure.

The rotation speed of high power low-speed marine diesel engine is 105 r/min. This speed should also be used when researching the exciting force from the cylinder gas pressure.

Due to the limited space, only the relative vibration displacement response between the propeller and crank 1 and crank 2 is presented as shown in Fig. 10. θ_1 and θ_2 represent the relative torsional angle between the propeller and crank 1 and the angle between crank 1 and crank 2 respectively. x_1 and x_2 represent the longitudinal vibration displacement between the propeller and crank and the displacement between crank 1 and crank 2 respectively, and so on.

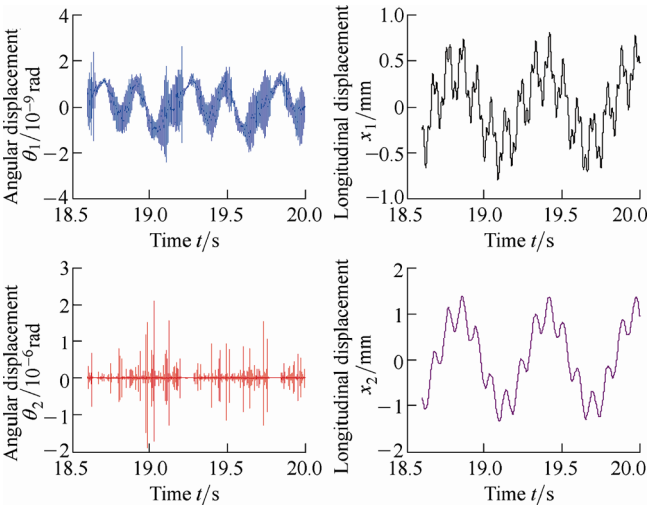

Fig. 10. Relative vibration response between propeller and crank 1, between crank 1 and crank 2

Comparing with the torsional vibration, the longitudinal vibration, which has various response components dominated with the dominant frequency component, has more obvious periodicity and regularity.

Although the external excitation applies on the rotation movement direction instead of directly on the longitudinal direction, the timing shows that torsional excitation could totally arise longitudinal vibration due to the coupled torsional-longitudinal factor. This longitudinal vibration is different from that of the torsional one in the aspect of response phase, response frequency with many super-harmonic and sub-harmonic components. The results can't be obtained through linear dynamic method, which emphasizes the importance of nonlinear dynamics.

Both in longitudinal vibration and torsional vibration, the system response components to the cylinder pressure are in fundamental frequency which means the vibration under such speed is normal and the propeller shafting system works stably.

Define excitation frequency ω_n divided by rotation speed of the crankshaft ω as disturbance frequency. Fig. 11 shows the spectrogram of the torsional vibration and longitudinal vibration in Fig. 10 in which the abscissa represents the ratio between response frequency and rotating frequency of the crankshaft, named frequency ration, and the ordinate represents the amplitude.

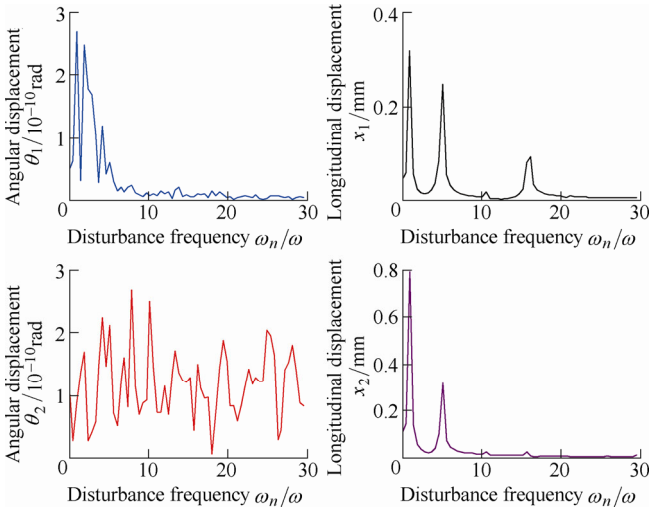

Fig. 11. Vibration spectrum between propeller and crank 1, between crank 1 and crank 2

Analysis shows that the relative torsional spectrums between the propeller and crank 1 and that between crank 5 and crank 6 include fundamental frequency, two times frequency, third times frequency rarely with other frequency. It shows obvious periodic behavior in time response while in the relative torsional vibration angular displacement spectrum between other cranks; it shows continuous spectrum which means the torsional vibration response involves many components which are very complicated.

For the longitudinal vibration, the frequency spectrums have nearly identical behavior with slight difference in the components and amplitude of all the frequency. The longitudinal vibration has fundamental frequency, 6 times frequency, 13 times frequency and 20 times frequency which is different from the torsional vibration spectrum. In the consideration of excitation caused by the vary of the gas pressure, only the first harmonic factors are considered while one torsional vibration period will cause 2 vibration period longitudinally due to the coupled torsional-longitudinal effect. Computing result proves that longitudinal vibration behavior is much complicated than the intuitive analysis with modeling.

According to spectrum analysis, other frequency components and fundamental frequency components are in

the same number range. The number of 6 times frequency component of the relative longitudinal vibration displacement between the propeller and crank 1 is even bigger than the fundamental frequency components. It is proved that during the design of the diesel engine propeller shafting system, it is not enough to base the strength calculation and vibration analysis on the linear dynamics research results, which will cause great error.

4.2.2 Response analysis at over-speed

The working speed of marine diesel with high power and low speed is 105 r/min. Considering the velocity variation caused by accidental factors, it is meaningful to research the response behavior under the speed of 130 r/min.

Under the speed of 130 r/min, the time response, phase diagram and spectrogram of torsional and longitudinal vibration is similar to that of 105 r/min. Fig. 12 shows the spectrogram under the speed 130 r/min.

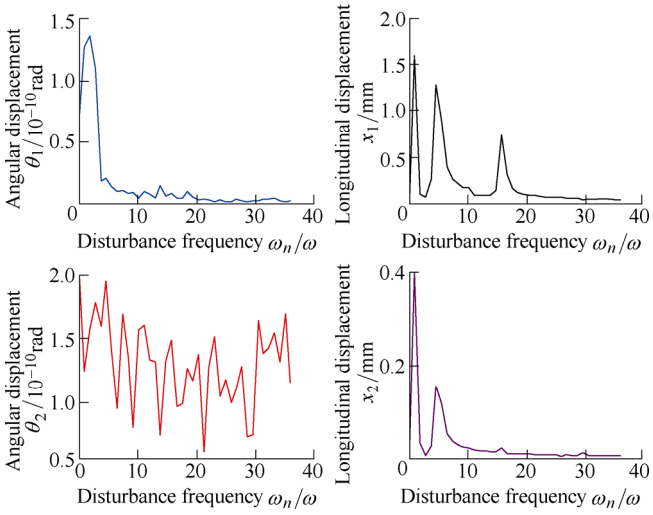

Fig. 12. Vibration spectrum between propeller and crank 1, between crank 1 and crank 2

From the spectrogram, it can be seen that the differences of the response behavior under the speed of 105 r/min and 130 r/min are mainly in the components of all frequency and the relative amplitude variations. In the torsional vibration spectrum between propeller and crank 1, the biggest amplitude is in 2 times frequency under 105 r/min while it is in fundamental frequency under the speed of 105 r/min. In the longitudinal vibration spectrum between the propeller and crank 1, the biggest amplitude is in 6 times frequency under the speed of 105 r/min while it is in fundamental frequency under the speed of 130 r/min. The 6 times frequency and 20 times frequency under the speed of 105 r/min are replaced with 5 times frequency and 15 times frequency.

For the amplitude, it varies little in the entire harmonic component under the speed of 105 r/min and 130 r/min, so is the amplitude in time response. All these prove that this propeller shafting system is safe and stable without abnormal vibration pheromones even over speed 20%.

4.3 Response by interaction of gas and fluid excitation

4.3.1 Response analysis at working speed

In the investigation of system response under the interaction of cylinder pressure and propeller hydro-oscillation excitation, assume that propeller mass, moment of inertia, torsional stiffness and other physical and mechanical properties are the same as that in section 3.1. Due to 4 rotor blades, the torque excitation frequency loaded on the propeller is 4 times as much as crankshaft speed even the fundamental frequency considered. That is to say, there is 4 times frequency excitation when considering propeller hydro-oscillation excitation.

Time histories of torsional and longitudinal vibration under the interaction of cylinder pressure and propeller hydro-oscillation excitation are shown as in Fig. 13.

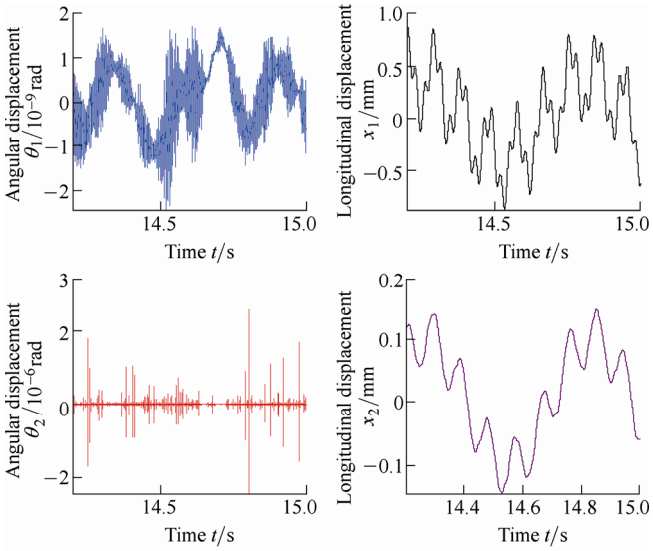

Fig. 13. Interactive excitation response between the propeller and crank 1, between crank 1 and crank 2

The torsional vibration behaviors between the propeller and crank 1 are nearly identical to that when only cylinder pressure is considered except for some difference in variations of high frequency harmonic components, and the amplitude of the former is smaller. For the relative vibration behaviors between the rests of the cranks, there are increased torsional vibration amplitude, decreased longitudinal vibration amplitude and nearly identical time response. Maximum amplitude between crank 5 and 6 is barely changed, but the amplitude of the other frequencies superimposed on the fundamental frequency is much larger. Furthermore, for the longitudinal vibration between crank 1 and crank 2, vibration amplitude under interactive excitation has few variations except for the relative amplitude of the harmonic components.

Above analysis shows that we can see that the behaviors and amplitude of the relative torsional and longitudinal vibration between cranks which are close to the propeller exhibit considerable variation, but variation behaviors between cranks close to sprocket is not relatively obvious.

Under the interaction of cylinder pressure and propeller hydro-oscillation excitation, why does the propeller-crankshaft system exhibit such behaviors? When the propeller hydro-oscillation excitation is transmitted to cranks through intermediate shaft, the torsional and longitudinal stiffness of the intermediate shaft is much bigger than that between cranks. In some given conditions, especially given speed, the excitation frequency on the propeller is far away from the natural frequency of the system. Consequently the propeller excitation causes little impact on crankshaft system vibration, which just arise amplitude variation of harmonic components and amplitude increase of torsional vibration without essential influences. Amplitude calculation without consideration of hydro-oscillation excitation is apt to have errors.

Fig. 14 shows the system spectrogram corresponding to Fig. 13. Under the interaction of cylinder pressure and propeller hydro-oscillation excitation, the relative torsional vibration response spectrum between the propeller and crank 1 contains the components of 2 times frequency and its amplitude is smaller than that cylinder pressure excitation act independently. There are no or few of 4 times excitation components loaded on the rotor blades, which is a rare phenomenon. For the longitudinal vibration spectrum, there are fundamental frequency, 6 times frequency and 20 times frequency components, and which is completely identical to that without the propeller hydro-oscillation excitation except for amplitude variations of all frequency components.

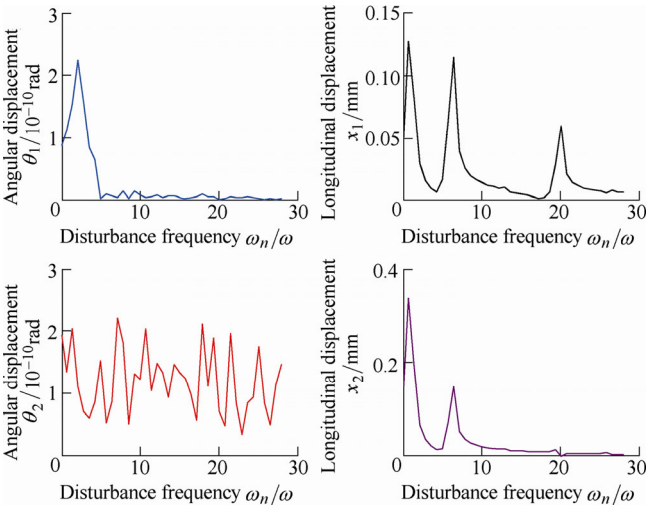

Fig. 14. Interactive vibration spectrum between the propeller and crank 1, between crank 1 and crank 2

Due to the complexity, there is no regularity to describe torsional vibration spectrum containing various frequency components. For the longitudinal vibration spectrum，there is no variation and the amplitudes of all frequency components decrease. Other frequency components of torsional and longitudinal vibration spectrum between the rest cranks have slight variations except for their amplitudes. Compared with the spectrum without propeller hydro-oscillation excitation, the torsional vibration spectrum just contains 2 times frequency components but fundamental frequency and 3 times frequency components.

From above spectrum analysis, the hydro-oscillation excitation arise only variations of all amplitudes corresponding to their frequencies. Considering all the spectrums, the number of the frequency components keeps stable and 4 times frequency components of propeller hydro-oscillation excitation never occurred or their amplitudes are much smaller than others', which is unique.

4.3.2 Over-speed response analysis

This section will research response spectrum at 130 r/min under the interaction of cylinder pressure and propeller hydro-oscillation excitation. Time response of the torsional and longitudinal vibration, phase diagram and spectrogram at 130 r/min is similar to that at 105 r/min. In order to save space, just spectrogram is given as Fig. 15.

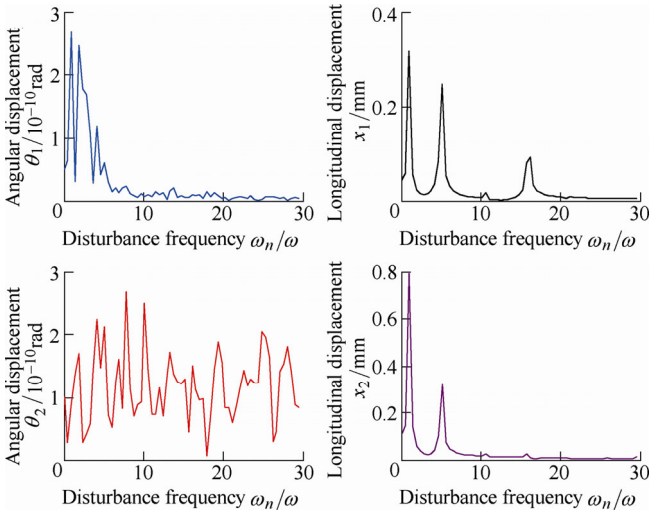

Fig. 15. Interactive excitation response between propeller and crank 1, between crank 1 and crank 2

As shown in Fig. 15, comparing with spectrum at working speed 105 r/min, the frequency components, including fundamental frequency, 5 times frequency, 10 times frequency and 16 times frequency, and its corresponding amplitude of relative torsional response between the propeller and crank 1 at speed 130 r/min increase. Obviously, it is different from that at 105 r/min. The longitudinal relative vibration spectrum containing fundamental frequency, 5 times frequency, 10 times frequency and 16 times frequency is different from the torsional vibration frequency components. And in comparison with spectrum at 105 r/min, all amplitude corresponding to their frequency components increase significantly, even including 4 times and 10 times frequencies.

Except for the relative torsional vibration behaviors between the propeller and crank 1, there is no much difference between 105 r/min and 130 r/min. Generally speaking, the torsional vibration frequency still has complex components.

With regard to longitudinal relative vibration at the speed

of 130 r/min, variations of the frequency components are not obvious, and their amplitude is almost doubled. Although running smoothly at the speed of 130 r/min, the system is sensitive to speed variations. For example, 20% increase in speed will lead to more than double of the amplitude of longitudinal vibration response, which should be paid much attention.

4.4 Discussion

Comprehensive influences evoked by multiple factors such as propeller, variable mass moment of inertia of linkages and pistons, and coupling effect between torsional and axial vibration are considered in this paper while non-constant inertia and structural damping of shaft segments in Ref. [16]. According to Ref. [22], the frequency of longitudinal vibration activated by torsional excitation is twice the frequency of torsional vibration, so both forward and reverse torsion of crankshaft can lead to the longitudinal shrinkage. Obviously, the model in Ref. [16] can't animate the actual motion states.

As can be seen from the results of the simulation, there are 2 times frequency components and the others are very little which reveals obvious rules of periodic change. The relative torsional vibration spectrums between some cranks are continuous and contain various torsional vibration components, which is much more complicated than that in Ref. [16]. For the relative longitudinal vibration, there are some differences in the amplitude of each frequency component and the law of the spectrum is almost the same. Unlike the torsional vibration spectrum, there is fundamental frequency and different frequency components in the longitudinal vibration response. Only torsional vibration response of the crankshaft was analyzed in Ref. [16] involving no longitudinal vibration caused by coupled torsional-longitudinal effect of the crankshaft.

All in all, for the nonlinear vibration activated by coupled torsional-longitudinal effect, system dynamic behaviors are quite complicated, especially in the response frequency components, which is different from the kinetic model in Ref. [16]. Therefore, it is not enough to use only the results of the dynamic analysis for strength calculation and vibration analysis in the design of diesel engine crankshaft system, which can result in big error.

5 Conclusions

(1) When the system is running at the speed of 105 r/min and excited by the interaction of gas pressure and fluid, the frequency and amplitude of relative torsional and longitudinal vibration among cranks near the propeller produce larger changes. At the other end remote from the propeller and near the site of the chain, the change of vibration is relatively insignificant. The reason for the above-mentioned phenomena is that the intermediate shafts transferring fluid excitation to cranks are solid parts and its torsional stiffness and longitudinal stiffness are much larger than the torsional and longitudinal stiffness among cranks.

(2) When the system is running at the speed of 130 r/min and excited by the interaction of gas pressure and fluid, the relative torsional vibration between propeller and crank 1 is different from the one at the speed of 105 r/min, but the law between each other crank is not much different. For relative longitudinal vibration, the frequency components have almost no noticeable change, the amplitude of each frequency component of almost all are more than doubled. This shows that although running smoothly at the speed of 130 r/min, the system is very sensitive to the speed change.

(3) The phenomenon that 4 times of an exciting frequency acting on the propeller by fluid appears when the crankshaft speed is 130 r/min, while not yield at 105 r/min, reflects the operation complexity of the system, and also proves the stability and safety at 105 r/min. While the possible abnormal vibration at over-speed just needs to be vigilant.

(4) It is necessary to research the nonlinear dynamic characteristics of the propeller shafting to verify whether the abnormal vibration phenomenon will be appear or not at normal or abnormal working conditions. Thus, all abnormal vibrations could be avoided in design phase, and the failure causes could also be judged out during operation, maintenance, and examination and testing.

References

[1] DOREY S F. Strength of marine engine shafting[J]. *Trans. NEC. Instn.*, 1939, 55: 69–78.

[2] POOLE. The longitudinal vibration of diesel engine crankshaft[J]. *J. Mech. E.*, 1941, 146(4): 13–19.

[3] SHIMOYAMADA K, IWAMOTO S, KODAMA T, et al. A numerical simulation method for vibration wave forms of high-speed diesel engine crankshaft system[J]. *Society of Automotive Engineers Transactions*, 1991, 100 (3): 933–953.

[4] SMAILI A A, KHETAWAT M P. Dynamic modeling of automotive engine crankshafts[J]. *Mechanism and Machine Theory*, 1994, 29(7): 995–1006.

[5] KANG Y, SHEEN G J, TSENG M H, et al. Modal analysis and experiments for engine crankshafts[J]. *Journal of Sound and Vibration*, 1998, 214(3): 413–430.

[6] BRUSA E, DELPRETE C, GENTA G. Torsional vibration of crankshafts: effects of non-constant moments of inertia[J]. *Journal of Sound and Vibration*, 1997, 205(2): 135–150.

[7] ASHRAFIUON H, WHITMAN A M. Design optimization of variable stroke compressors to minimize vibration by using asymptotic analysis[J]. *Journal of Vibration and Control*, 1999, 5(3): 461–474.

[8] MURAWSKI L. Longitudinal vibrations of a propulsion system taking into account the couplings and the boundary conditions[J]. *Journal of Marine Science and Technology*, 2004, 9: 171–181.

[9] SUN J, GUI C L, PAN Z D, et al. Effect of lubrication status of bearing caused by crankshaft deformation on crankshaft strength for crankshaft-bearing system of internal combustion engine[J]. *Chinese Journal of Mechanical Engineering*, 2006, 42(10): 109–114. (in Chinese)

[10] SUN J, WANG Z H, GUI C L. Elastohydrodynamic lubrication analysis of crankshaft bearing considering crankshaft deformation under load and roughness surface[J]. *Chinese Journal of Mechanical Engineering*, 2009, 45(1): 135–140. (in Chinese)

[11] SUN J, CAI X X, LIU L P. On the elastohydrodynamic lubrication performance of crankshaft bearing based on the effect of whole engine block deformation[J]. *Industrial Lubrication and Tribology*, 2012, 64(1): 60–65.
[12] ZHANG X, YU S D. Torsional vibration of crankshaft in an engine-propeller nonlinear dynamical system[J]. *Journal of Sound and Vibration*, 2009, 319(1–2): 491–514.
[13] CHARLES P, SINHA J K, GU F, et al. Detecting the crankshaft torsional vibration of diesel engines for combustion related diagnosis[J]. *Journal of Sound and Vibration*, 2009, 321: 1171–1185.
[14] KHALED N, CHALHOUB N G. A dynamic model and a robust controller for a fully-actuated marine surface vessel[J]. *Journal of Vibration and Control*, 2010, 17(6): 801–812.
[15] LIANG X Y, WANG Y S, SHU G Q, et al. Identification of axial vibration excitation source in vehicle engine crankshafts using an auto-regressive and moving average model[J]. *Chinese Journal of Mechanical Engineering*, 2011, 24(6): 1022–1027.
[16] LIANG X Y, WEN Y H, SHU G H, et al. Longitudinal vibration source identification of engine crankshafts based on auto-regressive and moving average model and analytic hierarchy process method[J]. *Journal of Vibration and Control*, 2013, 19(8): 1–15.
[17] HUANG Y, YANG S P, ZHANG F J, et al. Nonlinear torsional vibration characteristics of an internal combustion engine crankshaft assembly[J]. *Chinese Journal of Mechanical Engineering*, 2012, 25(4): 797–808.
[18] BELLAKHDHARA B, DOGUIA A, LIGIER J L. A simplified coupled crankshaft-engine block model[J]. *Comptes Rendus Mecanique*, 2013, 341: 743–754.
[19] LEE S M, LEE D W, HA Y H, et al. A study on the influence of waviness error to a hydrostatic bearing for a crankshaft pin turner[J]. *Tribology Transactions*, 2013, 56: 1077–1086.
[20] LIN Q, MENG B, YANG Q H. Numerical analysis and study of crankshaft system hydrodynamic lubrication and dynamic coupling system[J]. *Applied Mathematics & Information Sciences*, 2013, 7: 313–321.
[21] ZHANG Hongtian, ZHANG Zhihua, WANG Lin, et al. Calculation of coupled axial and torsional shafting vibration of motorship using system matrix model[J]. *Ship Engineering*, 1994(5): 36–42. (in Chinese)
[22] DU Hongbing, CHEN Zhiyan, JING Bo. The mathematical model for the coupled torsional-axial vibration of internal combustion engine shaft system[J]. *Chinese Internal Combustion Engine Engineering*, 1992, 13(2): 66–74. (in Chinese)

Biographical notes

ZHANG Qinglei, born in 1973, is currently a professor at *University of Shanghai for Science and Technology* and a professorate senior engineer at *Shanghai Electric Group Co., Ltd , China*. He received his PhD degree from *Xi'an Jiaotong University, China*, in 2003. His main research interests include system simulation, 3D printing and FEA.
E-mail: qingleizhang@sina.com

DUAN Jianguo, born in 1980, is currently a professor at *Central Academe, Shanghai Electric Group Co., Ltd, China*. He received his PhD degree on mechanical manufacturing and automation in *Tongji University, China*, in 2013.
E-mail: caleb_duan@aliyun.com

ZHANG Suohuai, born in 1962, is currently a professor at *Shanghai Institute of Technology, China*. He received his PhD degree on mechanical design and theory in *Xi'an Jiaotong University, China*, in 2000. His main research interests include mechanical system dynamics, virtual manufacturing and 3D design.

FU Yumin, born in 1988, is currently an engineer at *Central Academe, Shanghai Electric Group Co., Ltd, China.* She received her master degree on mechanical engineering in *Xi'an Jiaotong University*, *China*, in 2013.
E-mail: fu_yumin@126.com